Electronic Supplementary Information

Ying Duan *[a,b], Chi Zhang [a,c], Dongsheng Deng [a], Dong Sui [a], Xiaohan Gao[c] and Yanliang Yang *[a]

a. Henan Key Laboratory of Function-Oriented Porous Materials, College of Chemistry and Chemical Engineering, Luoyang Normal University, Luoyang 471934, China. yangyli@mail.ustc.edu.cn

b. College of Food and Drug, Luoyang Normal University, Luoyang 471934, China. duanying@mail.ustc.edu.cn

c. School of Petrochemical Engineering, Liaoning Petrochemical University, Liaoning Fushun, 113001, China.

Methods for theoretical calculation:

The first-principles [1,2] was employed to perform all Spin-polarization density functional theory (DFT) calculations within the generalized gradient approximation (GGA) using the Perdew-Burke-Ernzerhof (PBE) formulation. The projected augmented wave (PAW) potentials was chosen to describe the ionic cores and take valence electrons into account using a plane wave basis set with a kinetic energy cutoff of 450 eV. Partial occupancies of the Kohn−Sham orbitals were allowed using the Gaussian smearing method and a width of 0.05 eV. The electronic energy was considered self-consistent when the energy change was smaller than 10^{-5} eV. A geometry optimization was considered convergent when the energy change was smaller than 0.05 eV $Å^{-1}$. The vacuum spacing in a direction perpendicular to the plane of the structure is 15 Å. The Brillouin zone integration is performed using 3×3×1 Monkhorst-Pack k-point sampling for a structure. Finally, the adsorption energies(Eads) were calculated as Eads= Ead/sub -Ead -Esub, where Ead/sub, Ead, and Esub are the total energies of the optimized adsorbate/substrate system, the adsorbate in the structure, and the clean substrate, respectively. The free energy was calculated using the equation:

$$G = E + ZPE - TS$$

where G, E, ZPE and TS are the free energy, total energy from DFT calculations, zero point energy and entropic contributions, respectively. In our calculation, the U correction had been set as 3.39 eV for Rh atoms in our systems.

Table S1 The conversion of BHMF on different catalysts.

Entry	Catalyst	Cat. (mg)	Conv. (%)	Distribution of products (%)				C.B. (%)
				HD	MDPO	HHD	Others	
1	Ru/C	10	100	1	1	52	46	54
2	Rh/C	10	85	2	13	69	16	86
3	Pd/C	5	99	6	68	19	7	93
4	Pt/C	5	88	2	2	23	73	36

Reaction conditions: BHMF (128.0 mg, 1 mmol), H_3PO_4 (4 mL, 0.5 mol L^{-1}), H_2 1 atm, 333 K. C.B.carbon balance.

Table S2 Effect of acids on the hydrogenation of BHMF on Pd/C and Rh/C[a].

Entry	Cat.	Acid	pH [b]	Conv. (%)	Selectivity (%)				C.B. (%)
					HD	MDPO	HHD	Others	
1		H_3PO_4	1.83	99	6	68	19	7	93
2	Pd/C	HCl	1.81	87	12	47	18	23	80
3		H_2SO_4	1.86	93	10	52	16	22	80
5		H_3PO_4	1.83	100	2	10	72	16	84
6	Rh/C	HCl	1.81	98	7	13	55	25	76
8		H_2SO_4	1.86	100	10	17	58	15	85

[a] reaction conditions: Pd/C (5 mg), BHMF (128.0 mg, 1 mmol), Acid (4 mL), H_2 1 atm, 333 K; Rh/C (10 mg), BHMF (128.0 mg, 1 mmol), acid (4 mL), H_2 1 atm, 363 K. [b] the pH was determined by a pH meter. C.B. carbon balance.

Table S3 The content of metal in the sample determined by ICP-OES .

Entry	Catalyst	Metal content (wt.%)
1	Fresh Pd/C	5.04
2	Spent Pd/C	4.85
3	Fresh Rh/C	4.97
4	Spent Rh/C	4.86

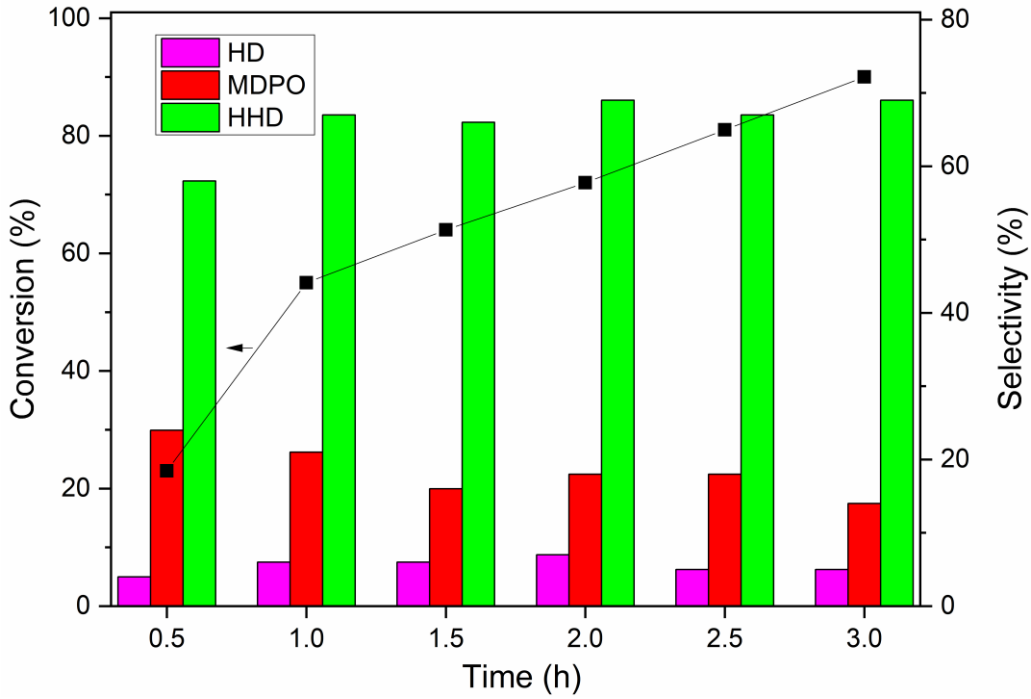

Figure S1 Effect of reaction time on the hydrogenation of BHMF on Rh/C.

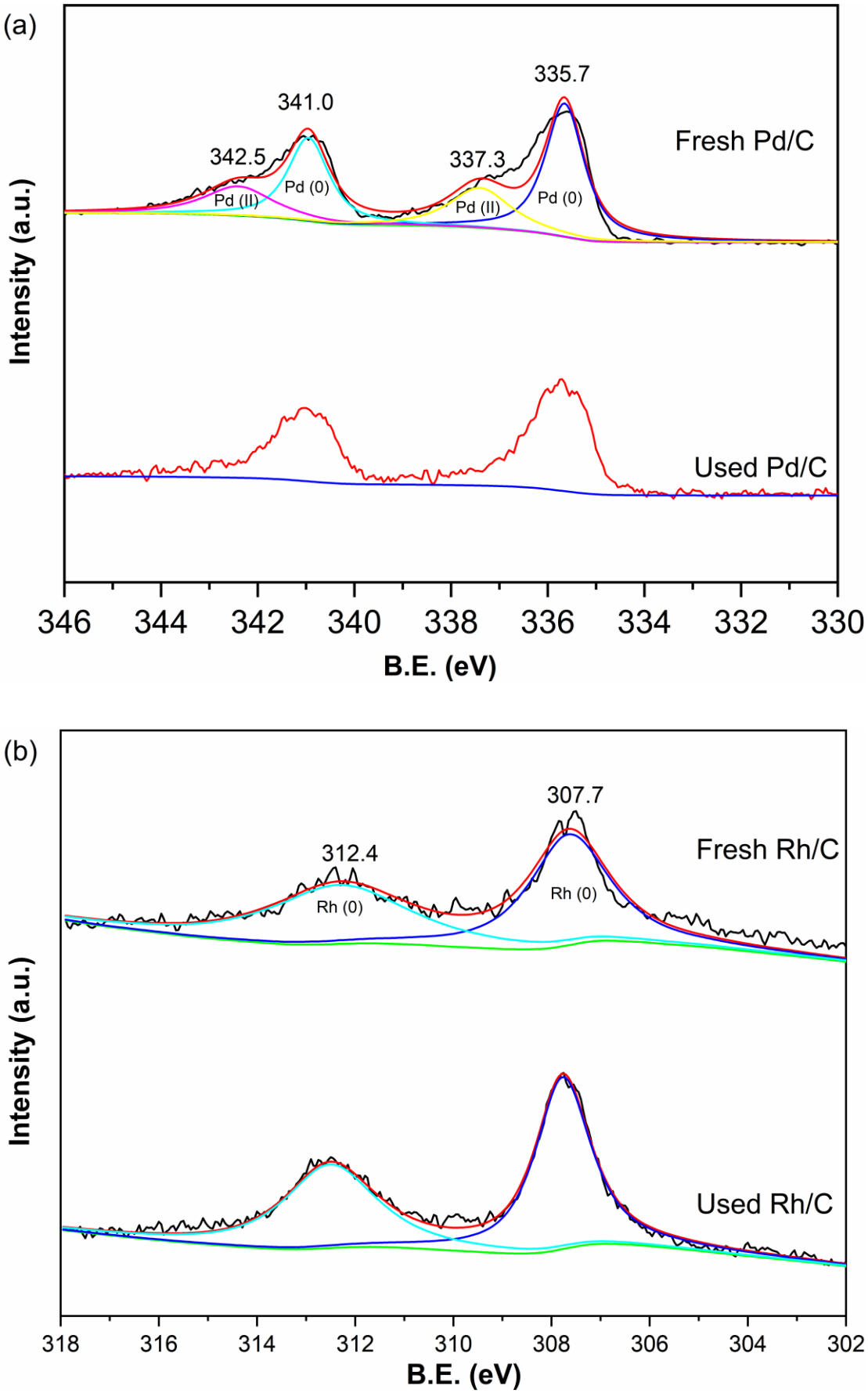

Figure S2 The XPS spectra for Rh and Pd on fresh and used Pd/C (a) and Rh/C (b)

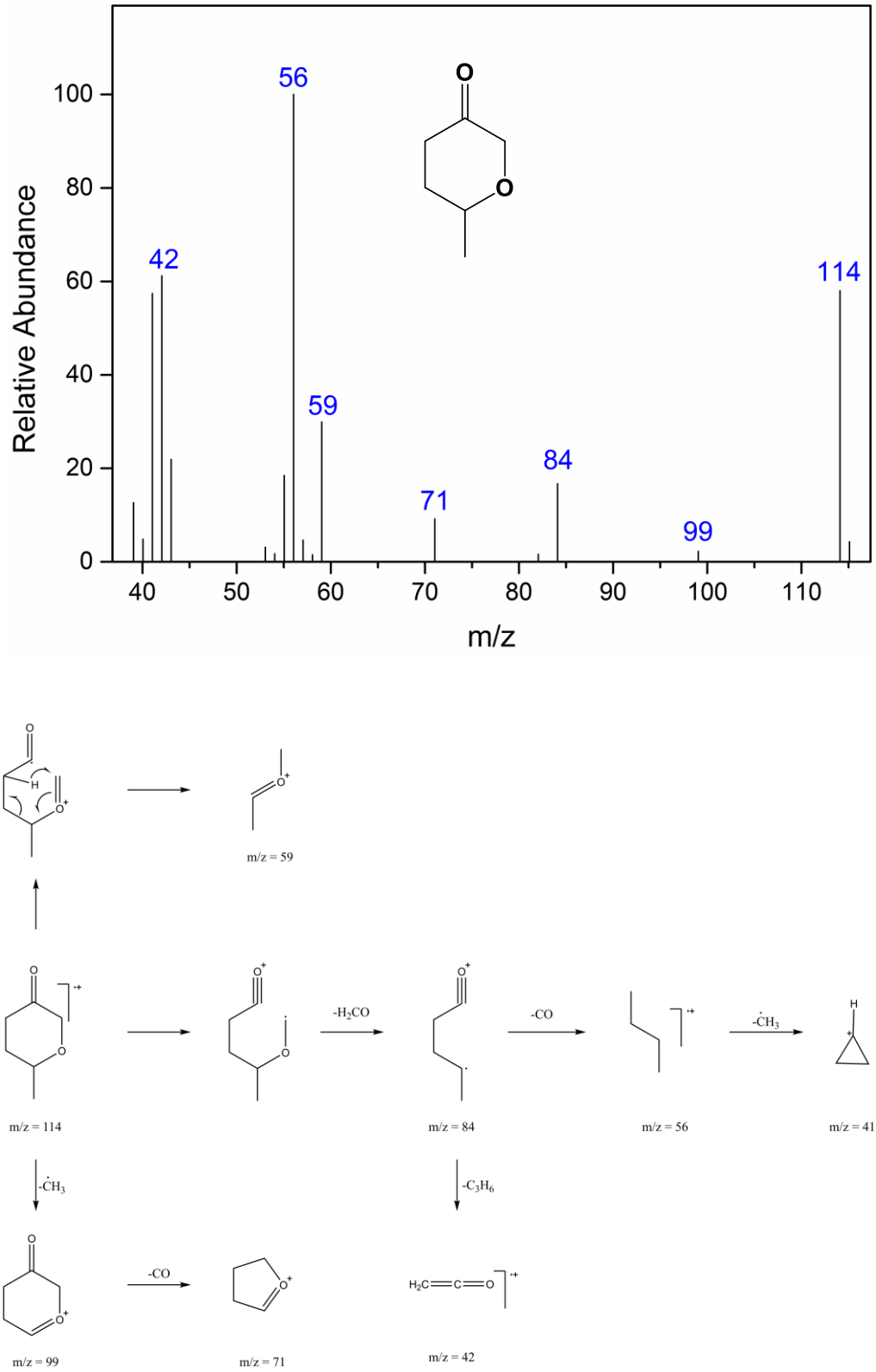

Figure S3 The mass spectra and ion fragments for MDPO.

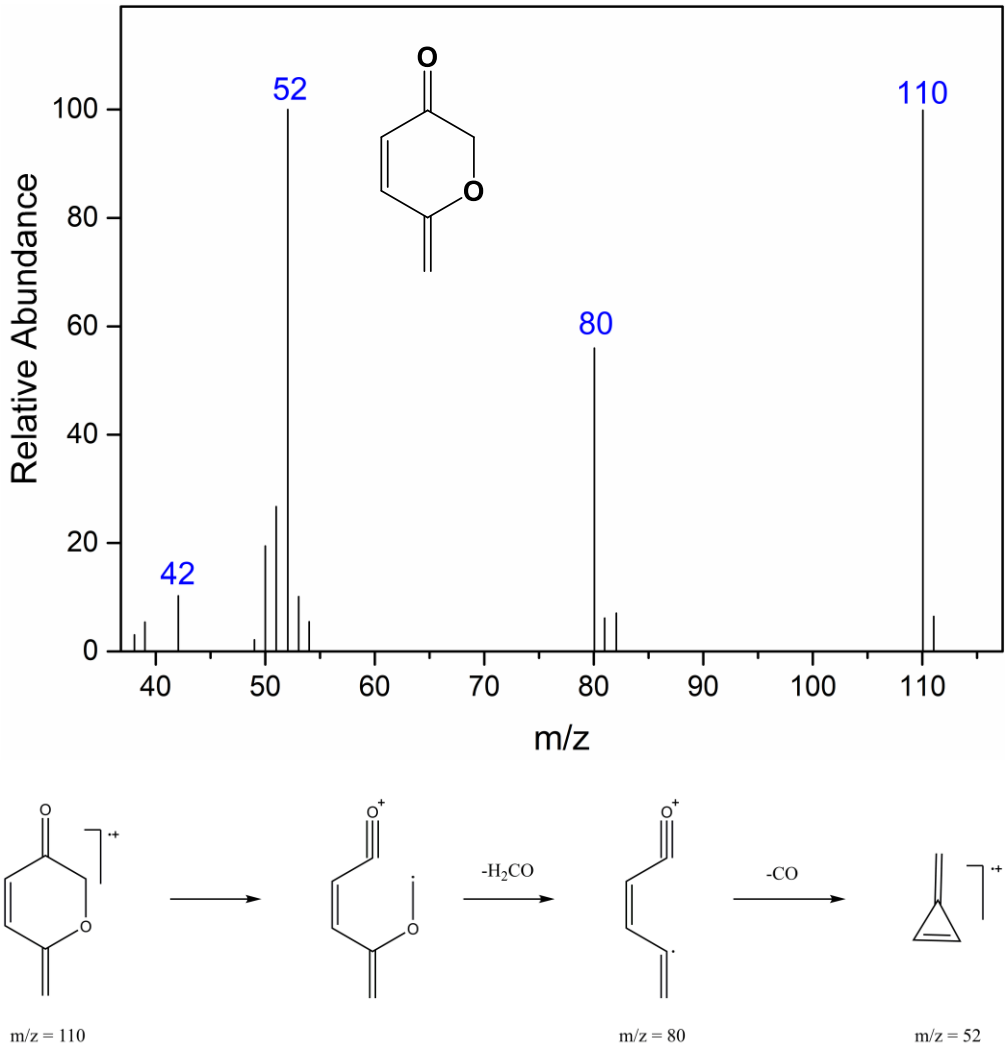

Figure S4 The mass spectra and ion fragments for MEPO.

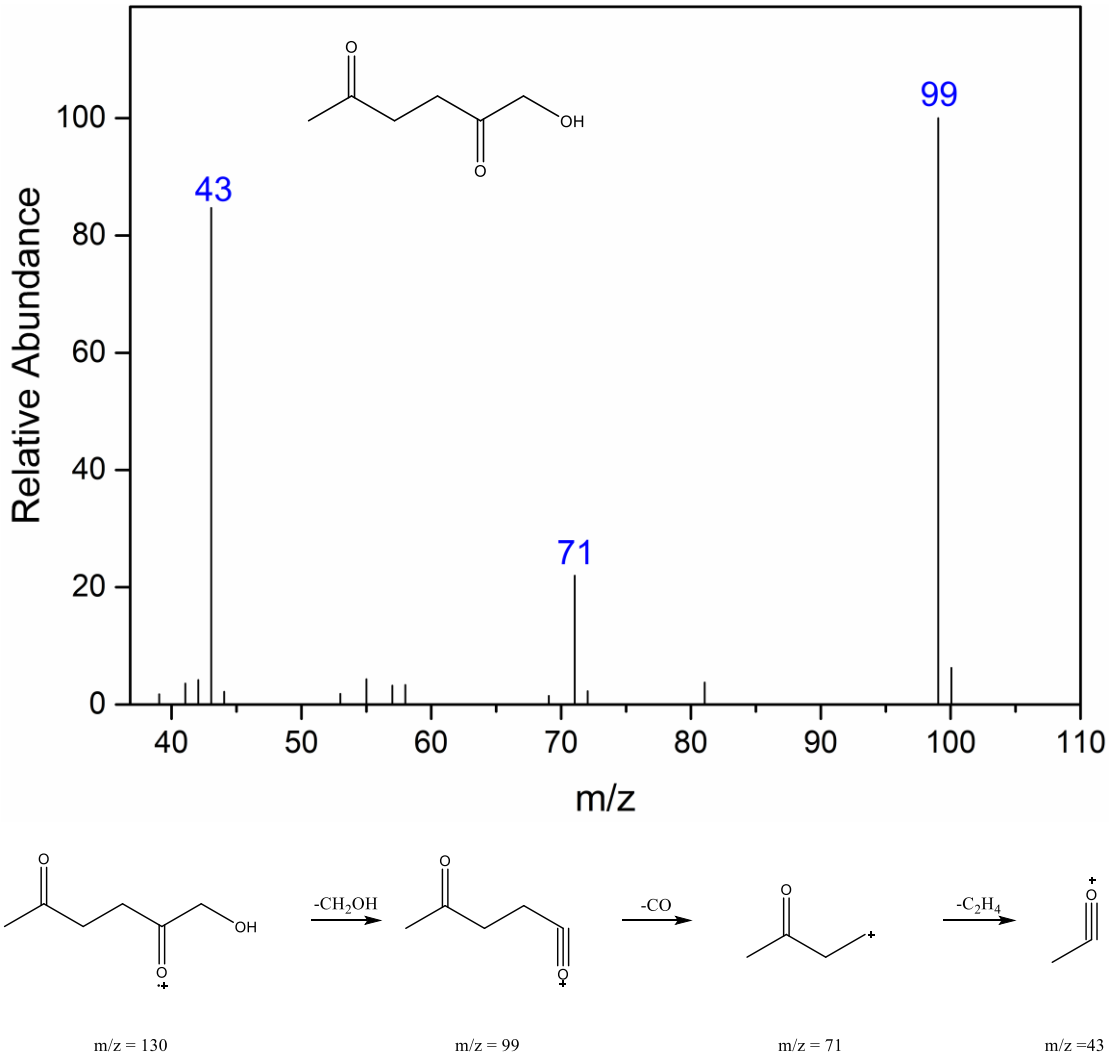

FigureS5 The mass spectra and ion fragments for HHD.

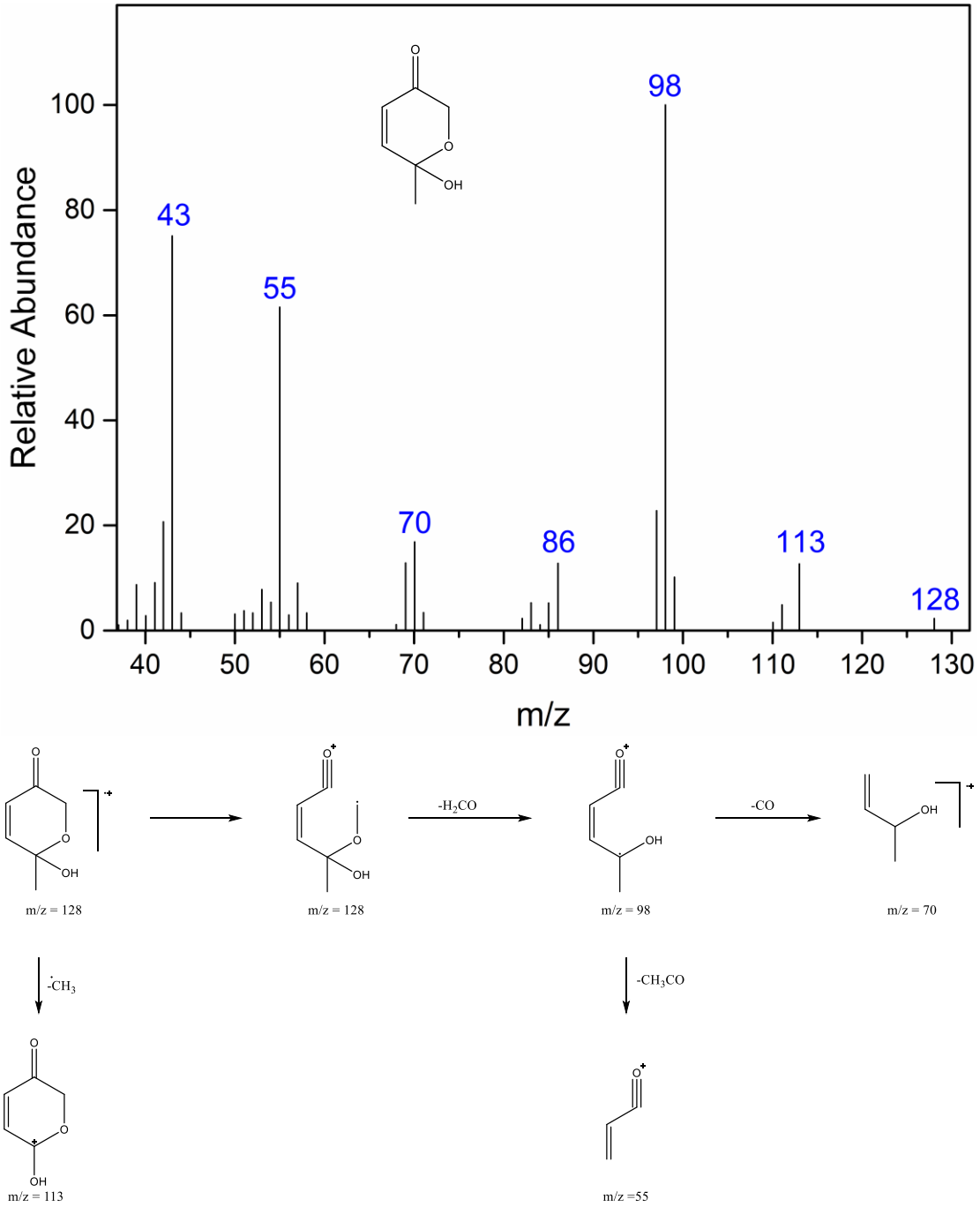

FigureS6 The mass spectra and ion fragments for HMPO.

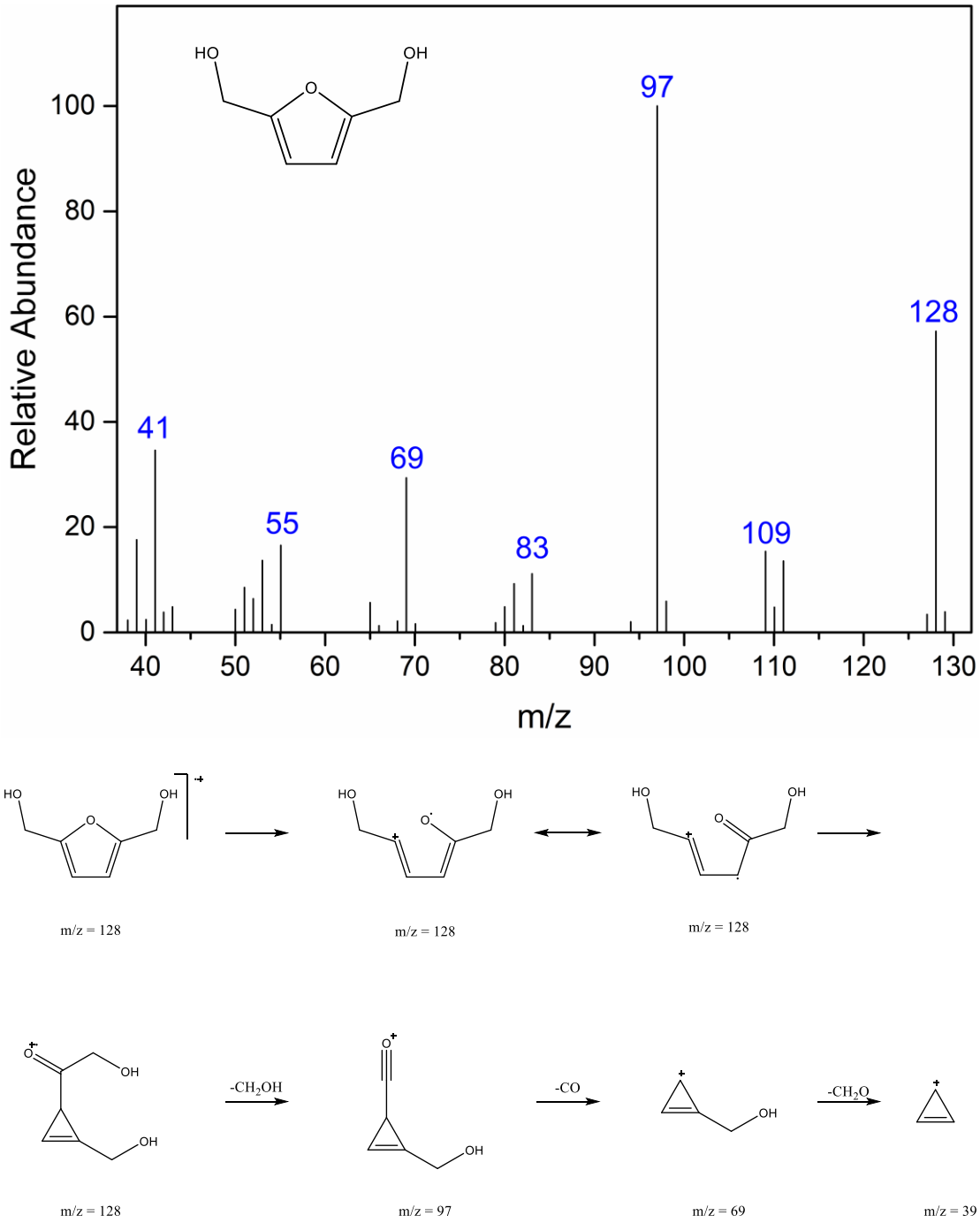

FigureS7 The mass spectra and ion fragments for BHMF

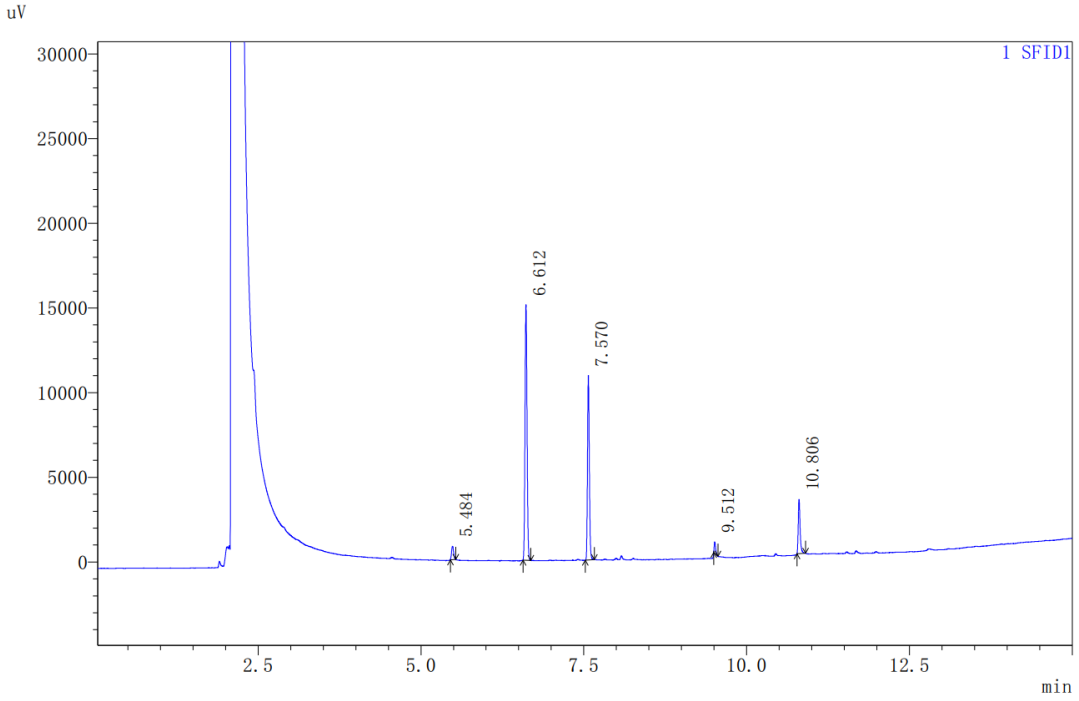

FigureS8 The GC trace for hydrogenation of BHMF on Pd/C (t = 6.61 min, internal standard; t = 7.57 min, MDPO; t=10.81 HHD).

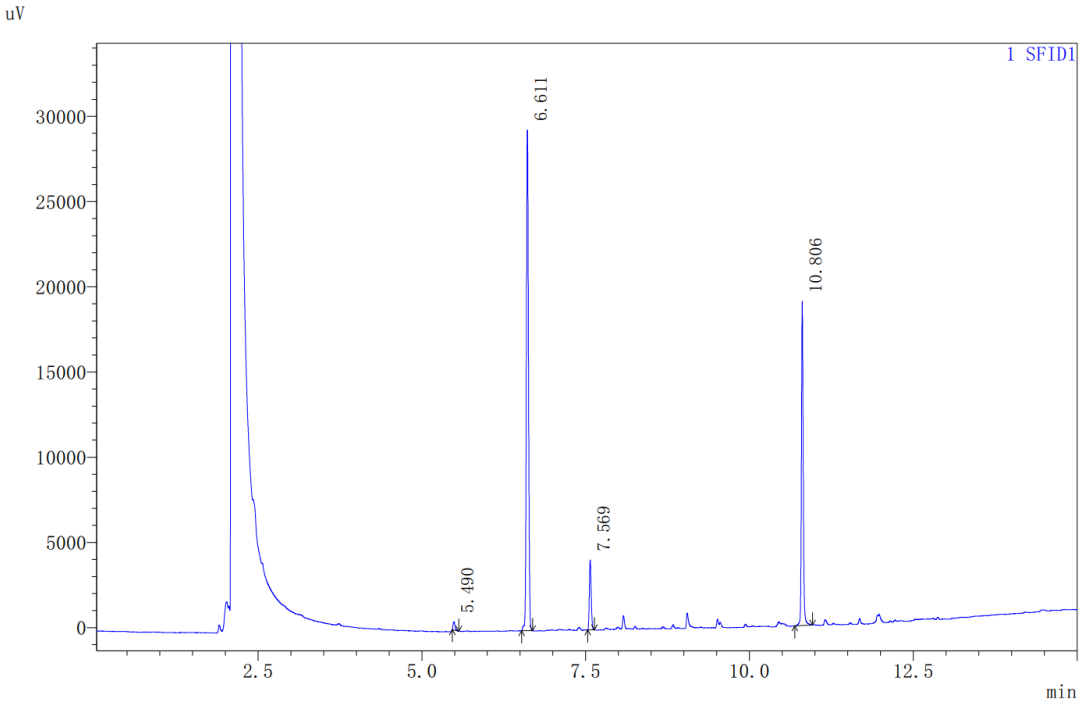

FigureS9 The GC trace for hydrogenation of BHMF on Rh/C (t = 6.61 min, internal standard; t = 7.57 min, MDPO; t=10.81 HHD).

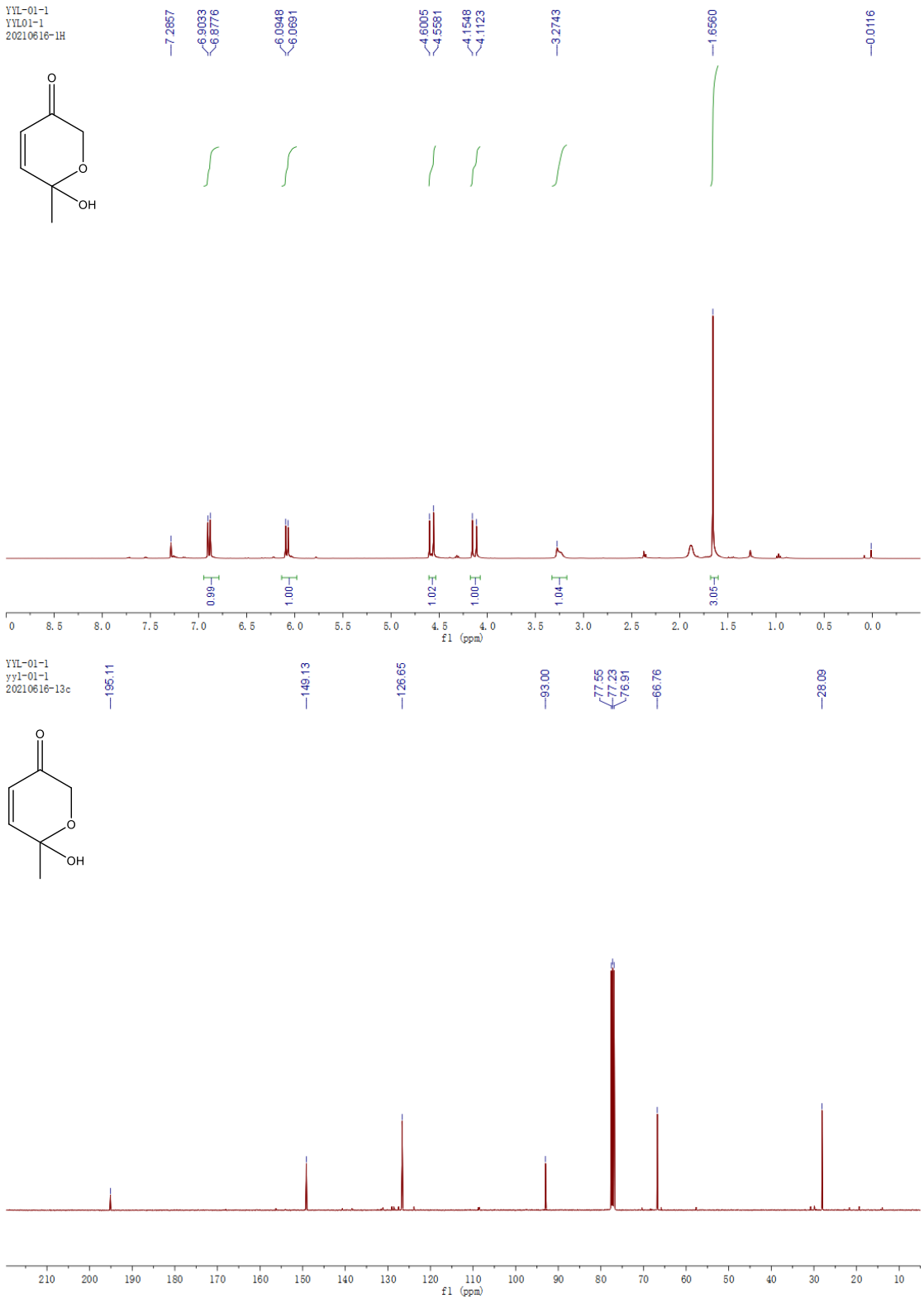

Figure S10 The ^{1}H and ^{13}C NMR spectra for HMPO.

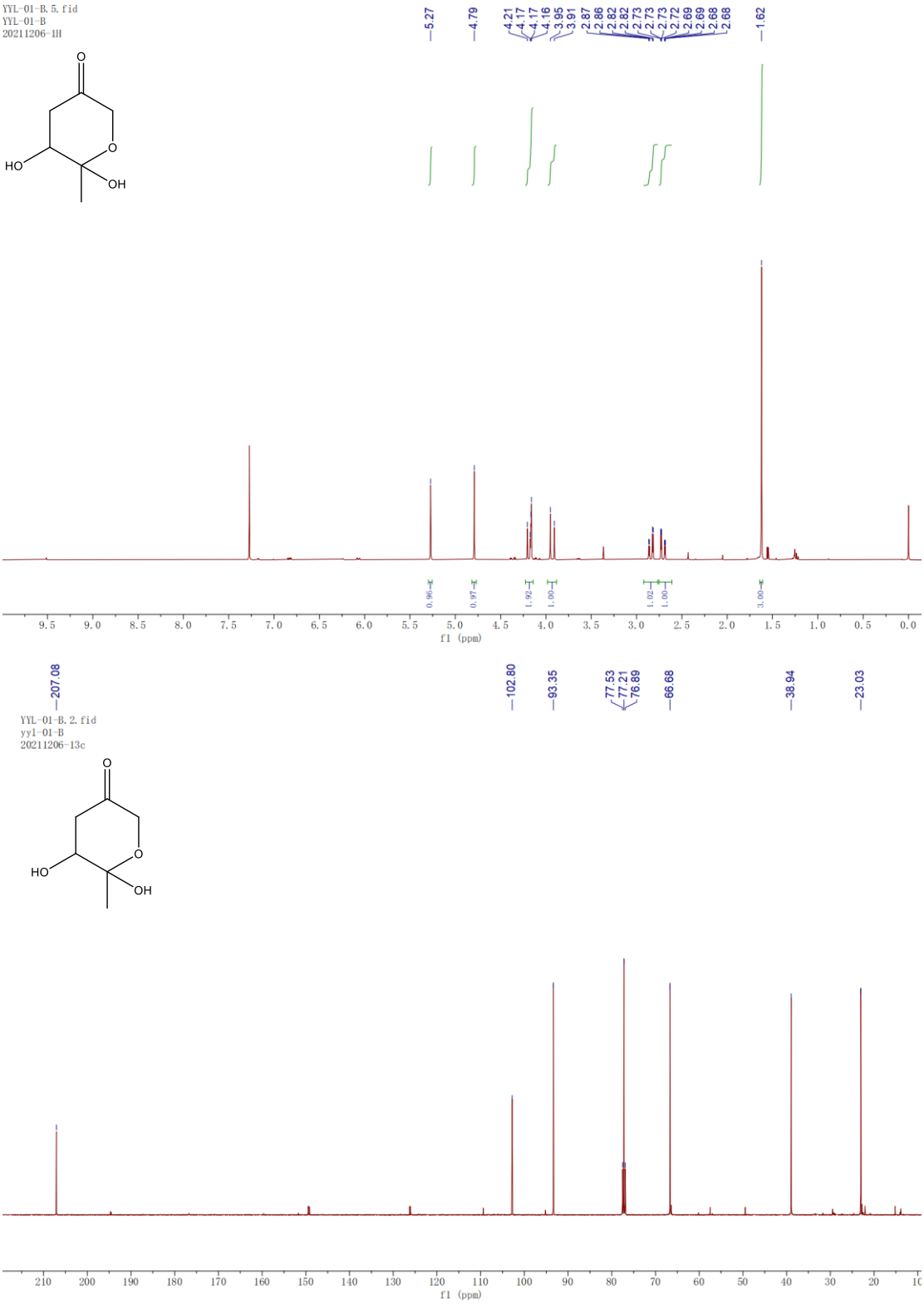

Figure S11 The ^{1}H and ^{13}C NMR spectra for DHDOP.

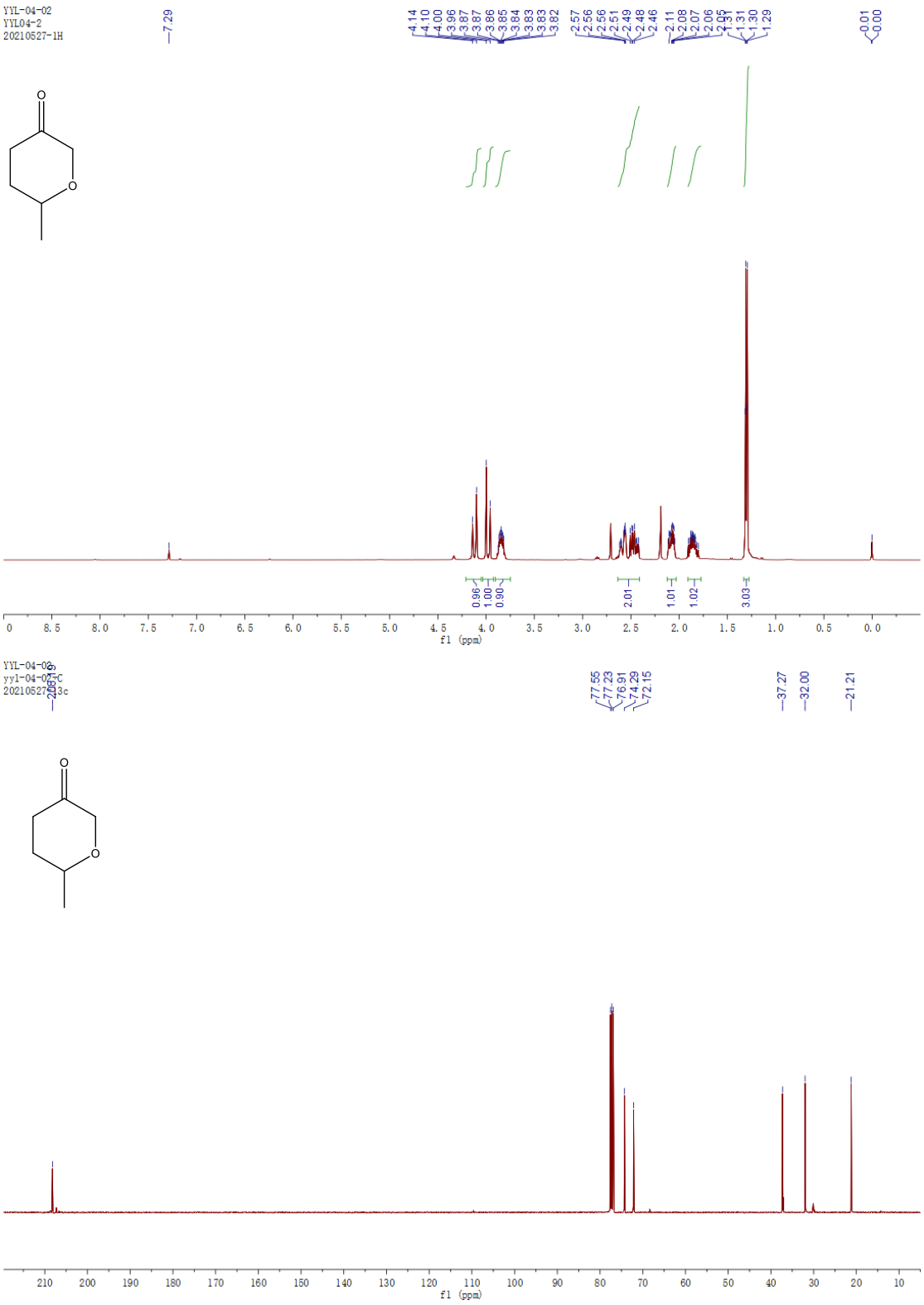

Figure S12 The ^{1}H and ^{13}C NMR spectra for MDPO.

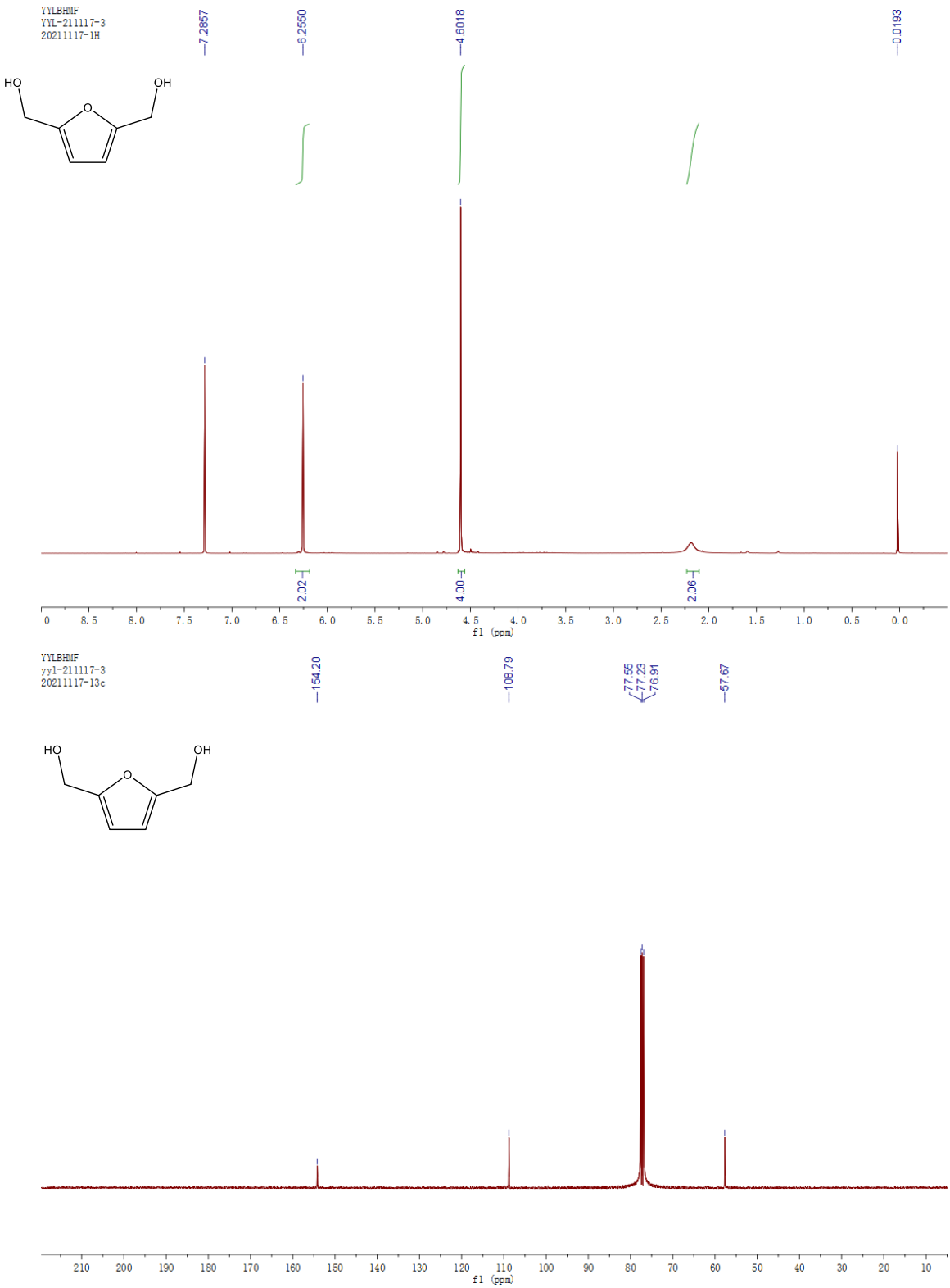

Figure S13 The ^{1}H and ^{13}C NMR spectra for BHMF.

Figure S14 The ^{1}H and ^{13}C NMR spectra for HHD.